Catalysis Letters 70 (2000) 83–91

Filamentous carbon templated SiO_2–NiO aerogel: structure and catalytic properties for direct oxidation of hydrogen sulfide into sulfur

Marina A. Ermakova *, Dmitriy Yu. Ermakov, Max Yu. Lebedev, Nina A. Rudina and Gennadiy G. Kuvshinov

Boreskov Institute of Catalysis, Prosp. Ak. Lavrentieva 5, Novosibirsk 630090, Russia
E-mail: erm@catalysis.nsk.su

Received 4 April 2000; accepted 11 September 2000

Silica aerogels comprising nickel oxide nanoparticles were synthesized with no use of supercritical drying. A high specific surface area (more than 1000 m^2/g), mesoporous structure and considerable stability to sintering up to 900 °C are characteristic of these aerogels. The aerogels were synthesized using the sol–gel method. Filamentous carbon was templated by silica, tetraethoxysilane being used for supplying silica. Carbon was burnt later. Analysis of the aerogel structure revealed the presence of silica nanotubes and nanofibers. Aerogel testing for direct oxidation of H_2S into S^0 demonstrated as high as 60% conversion of hydrogen sulfide at almost 100% selectivity under stoichiometric conditions at the temperature range of 300–350 °C and 73% conversion at 100% selectivity at a considerable excess of oxygen at 160 °C.

Keywords: filamentous carbon, silica aerogol, sol–gel method, hydrogen sulfide direct oxidation

1. Introduction

Silica is one of the oxide materials which are the most practical in industry. Both silica and silica-based composites are used. The polymerizability of silicic acid in the form of reticular structures is employed for sol–gel syntheses. A sol–gel synthesis allows silica-containing species to be deposited onto various templates in order to produce an oxide material with an unconventional internal structure. Surfactants [1] and carbon-containing materials [2] are used as the templates.

Tetraethoxysilane (TEOS) is mostly used for supplying high-purity silica for sol–gel syntheses. Depending on the conditions, TEOS undergoes hydrolysis to form a polyethoxysilane solution (acidic hydrolysis) or a sol comprising silica particles (alkaline hydrolysis). The further drying of the hydrolyzate results in formation of a solid xerogel with the textural parameters depending on the conditions of hydrolysis and drying [3–6]. Numerous researchers introduce metal salt solutions at the stage of hydrolysis in order to obtain dense or porous composite materials, in which metal or metal compound particles would be uniformly allocated through the xerogel bulk [7–12]. Sometimes this method is used for designing catalytic systems to provide reliable sintering protection of active metal nanoparticles [13,14].

Our previous study [15] was focused on various carbon materials to be used as templates for synthesis of porous silica. TEOS was subjected to pre-hydrolysis in the presence of an acid and water in a substoichiometric amount; the obtained solution was introduced into pores of a carbon matrix. TEOS was condensed in the pores as the solvent was evaporated. The further thermal treatment resulted in formation of solid silica-containing films on the carbon surface. The carbon was eliminated (gasified as carbon dioxide) by means of oxidative thermal treatment with air at 600 °C. Xerogels with various textural parameters were synthesized. The most striking internal structure was characteristic of the xerogels synthesized using catalytic filamentous carbon (CFC) as the carbon pore-forming matrix.

CFC is formed upon catalytic decomposition of hydrocarbons and carbon monoxide at 400–750 °C. Nickel [14, 16,17], iron [18,19] or Ni–Fe alloys [20] and, sometimes, cobalt [21,22] catalyze this process. Various CFC modifications, from a loose powder to solid mesoporous granules, can be produced depending on the catalyst and reaction conditions. EM studies show that the CFC structure is built up by interlaced carbon nanofibers or nanotubes with a metal particle at the tip. It is known that the metal particle should be, preferably, 10–60 nm in size to provide the carbon filament growth. The filament diameter equals the diameter of the catalytic particle. The hydrocarbon decomposition proceeds on specific edges of the catalytic particle, and the deposition of the graphite-like carbon on the others [24,25]. The catalyst lifetime being rather long, up to dozens of hours, the carbon nanofibers can reach 10–15 μm length.

In the present article we consider in detail a SiO_2–NiO aerogel, which was synthesized using carbon nanofibers with catalytic particles in the tips as the template.

* To whom correspondence should be addressed.

Since this material possesses a high specific surface area, open porous structure and, additionally, includes dispersed nickel oxide, it seems to be a promising catalyst for oxidative reactions. We used direct oxidation of hydrogen sulfide into sulfur as the test reaction. This process continues to be of interest to researchers because of severe requirements to admissible H_2S concentration in waste gases of various industries. It is known that materials with high surface areas, such as activated carbons or metal oxides, are used as catalyst for direct oxidation of hydrogen sulfide into sulfur. Activated carbons are employed at low temperatures (20–120 °C) and near to stoichiometric $O_2 : H_2S$ ratio (or at small excess of oxygen) [26]. Activated carbons are considered to reveal a strong resistance against water [27]. Apart from the carbons, nickel oxide [28] or copper oxide [29] can be used at this temperature range. A drawback of these catalysts is that sulfur is accumulated on the active surface under the reaction conditions to cause the necessity of the catalyst regeneration in certain periods of time. It is inappropriate to elevate the temperature, because considerable amount of SO_2 is formed among the reaction products. For this reason, preferable are catalysts operating at higher temperatures (160–300 °C), i.e., under the conditions excluding sulfur condensation in the reaction zone. These are oxides of iron [30], chromium [31], titanium [32], etc. The oxides may be used as they are or as supported on an appropriate carrier, typically SiO_2. A high selectivity to sulfur is characteristic of these catalysts at high temperatures.

It was found earlier [32] that bare silica reveals a low activity to the direct oxidation of hydrogen sulfide into sulfur, probably because of a low surface area of the available silica, as well as of the insufficient surface exposure to the reactants due to the absence of transport pores. We used SiO_2 aerogel prepared by templating a matrix of pure carbon material (Sibunit), which possessed a high specific surface area and large pore volume, for comparative studies.

2. Experimental

Tetraethoxysilane (TEOS) hydrolyzed by a substoichiometric amount of water in an acid medium was used for experiments. The hydrolyzate was prepared by mixing 50 ml of TEOS, 40 ml of ethanol, 2 ml of water and 0.5 ml of 40% HCl. After drying and calcination in air at 600 °C, the hydrolyzate contained 0.147 g of dry residue per 1 ml of the solution. The prepared hydrolyzate was aged at room temperature for 72 h. Carbon samples were impregnated by the hydrolyzate (in excess liquid phase) during 1 h. It was experimental observation that a longer impregnation procedure (up to 72 h) did not result in an increase in the sample weight after drying. Therefore, it was assumed that the equilibrium was established during the first hour but no adsorption from the solution occurred later. The excess hydrolyzate was poured off. Carbon was dried at room temperature for 24 h, calcined at 300 °C for 1 h, weighed, and then eliminated by burning in air at 600 °C.

CFC prepared by catalytic decomposition of methane was used as templates for synthesis of the oxide material. Catalysts were Ni–SiO_2 systems comprising 90% of nickel [14]. The catalysts were carbonized during 6 h (loose carbon) and 40 h (dense carbon) in order to vary textural parameters of CFC and the weight ratio (ca. 1.5 and 0.3% Ni, respectively).

Bare silica aerogel was used for comparative studies of the oxidation power for direct oxidation of hydrogen sulfide into sulfur. It was prepared by the same procedure as that for the SiO_2–NiO sample except Sibunit (a pure mesoporous carbon material synthesized by depositing pyrocarbon on carbon black followed by activation [33]) was used as the matrix.

The amount of SiO_2 deposited on carbon was varied by diluting the primary hydrolyzate with ethanol or changing the number of impregnation procedures. If the number of impregnation procedures were more than one, the whole cycle except the carbon burning was repeated as many times as needed. The amount of SiO_2 deposited on carbon was estimated as grams of SiO_2 per gram of carbon.

Textural parameters of carbon matrices and of silica obtained upon carbon burning were studied by low-temperature nitrogen adsorption at 77 K using an automated installation ASAP-2400.

X-ray powder diffraction patterns were recorded using a URD-63 diffractometer (Cu K_α radiation at $\lambda = 0.15418$ nm, a graphite crystal monochromator). Silicon was used as an internal reference. Coherent scattering regions for nickel oxide were determined by the Scherer equation [34] based on broadening of diffraction lines (111) and (200) for NiO.

IR spectra were recorded at 400–2000 cm^{-1} using a spectrometer Shimadzu 8300. KBr was used as filler.

Micrographs were recorded using a transmitting electron microscope JEM-2010.

Aerogel samples were tested in direct oxidation of H_2S into sulfur using an ideal mixing microreactor with a fluidized catalyst bed at 160–400 °C and atmospheric pressure. An inlet gas mixture was prepared by mixing hydrogen sulfide, nitrogen and air in the required proportions. The inlet concentration of H_2S was varied from 0.4 to 1% depending on the reaction temperature. The reaction was conducted at either stoichiometric or 16% concentration of oxygen. The reaction mixture consumption was 60 cm^3/min. Samples in amount of 0.1 g were loaded. The microreactor was a quartz tube of 15 mm diameter and 100 mm height with a gas distribution grid sealed in it; a sample bed to be studied was poured over it. The reactor was enclosed into a thermostat with the temperature maintained using electric heating spirals. Sulfur generated by the reaction was accumulated in a condenser at the reactor output. If the reaction temperature was varied, the activity and selectivity were determined for the catalyst left under these conditions for 10 h. The feed and the gas products were analyzed

chromatographically using a Porapak column. Testing was stopped after 20 h under the reaction conditions.

The conversion of the hydrogen sulfide and selectivity to sulfur were calculated using equations:
conversion (%)

$$X = \frac{[H_2S]_{inlet} - [H_2S]_{outlet}}{[H_2S]_{inlet}} \times 100,$$

sulfur selectivity (%)

$$S = \frac{[H_2S]_{inlet} - [H_2S]_{outlet} - [SO_2]_{outlet}}{[H_2S]_{inlet} - [H_2S]_{outlet}} \times 100.$$

3. Results and discussion

3.1. Structure and properties of CFC

A typical process of methane decomposition to produce CFC is conducted in a fluidized catalyst bed. Such a process arrangement is needed to prevent conglutination of growing CFC granules. Otherwise, a dense carbon cork is formed impeding the normal gas passage through the reactor. The process of CFC granule growth in the fluidized catalyst bed is discussed in detail elsewhere [23]. Table 1 shows the results of textural studies of three samples of filamentous carbon prepared by decomposition of methane on the 90% Ni–10% SiO_2 catalyst. Different carbonization times (10, 15 and 35 h) and, consequently, different yields of carbon per gram of nickel (100, 150 and 300, respectively) are characteristic of these samples. Thus, it is seen that the longer is the process, the denser is the carbon and the lower is the pore volume. The nickel concentration in the carbon product is an important factor because all nickel becomes a constituent of the xerogel to be synthesized. The nickel content depends on the carbonization time of the initial catalyst and can be varied over a wide range. The lowest nickel content (<0.3%) is observed at the highest carbon yield. Besides, the nickel content in the carbon can be decreased using the acid treatment (table 2). The lowest nickel content is observed in the carbon treated with concentrated nitric acid. It should be noticed here that the carbon is also dissolved under these conditions to form the so-called graphitic acid, a total of weight loss being 11.4% during the experimental time. Unfortunately, we failed to eliminate all nickel from CFC, probably due to the fact that some Ni portion is dispersed through the bulk of carbon filaments and inaccessible to acid until the filaments are fully dissolved.

Table 1
Influence of carbon yield on textural parameters of CFC.

Carbon yield (g-C/g-Ni)	Specific surface area (m^2/g)	Pore volume (cm^3/g)	Average pore diameter (nm)
100	120	0.345	11
150	94	0.310	13
350	70	0.253	15

Thus, CFC synthesized over high-loaded Ni catalysts in the fluidized bed (figure 1 (a) and (b)) is a new granulated carbon, the structure and properties of which can be varied within certain range.

3.2. Textural parameters of aerogels as depended on preparation conditions and calcination temperature

The hydrolyzate prepared by partial hydrolysis of TEOS in an acid medium is the solution of linear polyethoxysilane molecules [3]. When the impregnation of a porous carbon by this solution is followed by the solvent removal, polyethoxysilane is condensed into gel, which decreases in volume to form an elastic film covering the surface of the carbon filaments. Pre-calcining at 300 °C results in elimination of a considerable portion of the organic constituent of the coat and chemisorbed water. The carbon is not oxidized due to the high level of graphitization, the oxidation does not start at a noticeable rate but at a temperature as high as 400 °C. Notice that the high graphitization level causes negligible proportion of micropores in the CFC texture, i.e., there is no site inaccessible to polymer molecules during impregnation. The adsorption data show indeed no change in the texture after impregnation of CFC by the hydrolyzate and preliminary calcination. This observation argues the high uniformity of the silica coat on the carbon surface. The further oxidative calcination at 600 °C for 5–6 h results in the complete burning of the filamentous carbon as well as the carbon constituent of the polysiloxane coat. The resulting structure is built up by porous silica and nickel dispersed through the bulk. A very light opalescent aerogel produced in such a way does not crumble into powder but retains the shape of the precursor, the carbon granule. Textural data on aerogel samples synthesized by depositing silica on CFC and Sibunit are summarized in table 3. Rather high specific surface areas at the mesoporous structure are seen to be characteristic of the samples. The pore volumes correspond to those of aerogels produced by supercritical drying [35].

The composite material synthesized as described above, even though it contains nickel in a substantial proportion, reveals a high sintering stability. Table 4 shows data on the specific surface area and total pore volume of aerogel synthesized by supporting 10 wt% of silica on CFC; they are seen not to change considerably (by no more than 18 and

Table 2
Influence of conditions of acid treatment during 60 h on the residual nickel content in CFC.

Medium of treatment	Temperature of treatment (°C)	Residual amount of nickel (%)
Empty	–	0.68
HCl 40%	Boiling point	0.55
HF 49%	Boiling point	0.47
HNO_3 concentrated	Boiling point	0.13
H_2SO_4 concentrated	90	0.48
H_3PO_4 concentrated	160	0.42

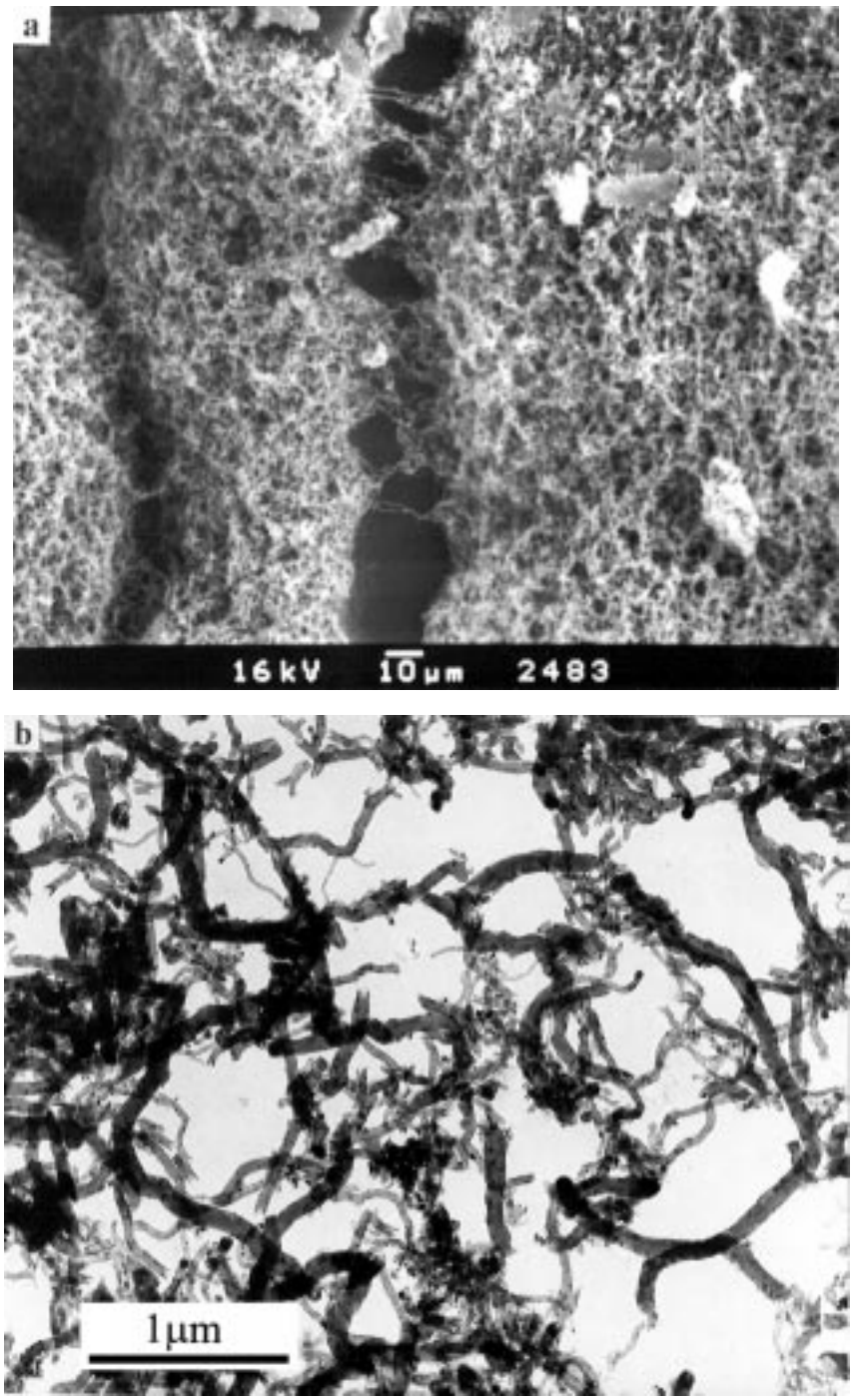

Figure 1. (a) Microscopic section of a granule of filamentous carbon produced by catalytic decomposition of methane and (b) typical carbon filaments growing on nickel catalysts in the methane atmosphere.

Table 3
Textural parameters of silica gel prepared by supporting SiO_2 in amount of 7% of carbon weight on CFC and Sibunit.

Carbon matrices	Textural parameters of silica after removing of carbon		
	Specific surface area (m^2/g)	Pore volume (cm^3/g)	Average pore diameter (nm)
CFC	1191	5.6	17.8
Sibunit	775	2.8	14.8

Table 4
Influence of calcination temperature on textural parameters of silica prepared by supporting SiO_2 in amount of 10% of carbon weight on CFC.

Calcination temperature (°C)	Specific surface area (m^2/g)	Pore volume (cm^3/g)	Average pore diameter (nm)
600	1087	4.19	15.84
800	912	3.97	17.4
900	893	3.8	20

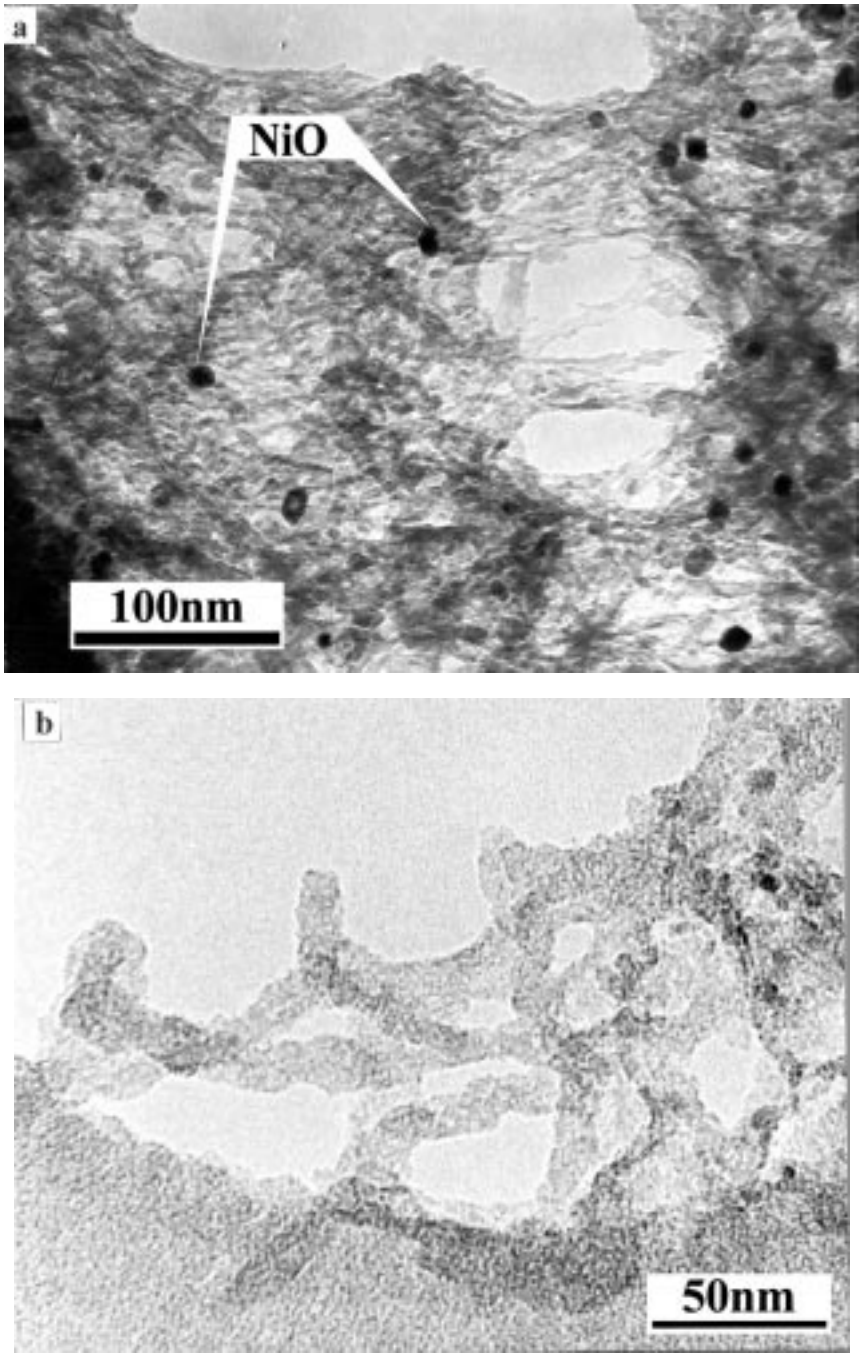

Figure 2. (a) Typical structure of aerogel synthesized by templating silica onto CFC at high carbonization level (150 g-carbon/g-nickel) and (b) silica nanofibers.

9%, respectively) upon 2 h calcination at 900 °C. Much higher sintering of silica is usually observed under these conditions. For example, Goodman et al. [36], who studied sintering of high-purity silica synthesized from TEOS, observed a decrease in the specific surface area from 750 to 450 m^2/g upon the 2 h calcination at 800 °C.

3.3. Aerogel structure

A typical structure, which is characteristic of most aerogels synthesized by templating silica on CFC with a high carbonization level (>60 g-C/g-Ni), is shown in figure 2(a). The aerogel is composed of extended thin-wall structures, which are silica coats of carbon filaments. Since the filaments are interlaced in rather close manner in the carbon granules (figure 1(a)), one can hardly distinguish any individual element in the aerogel structure, although individual silica species in the form of nanofibers may be seen sometimes (figure 2(b)). Probably, these species are the result of sintering of thin-wall coats after the very thin carbon filaments have been removed; in most cases no sintering proceeds though.

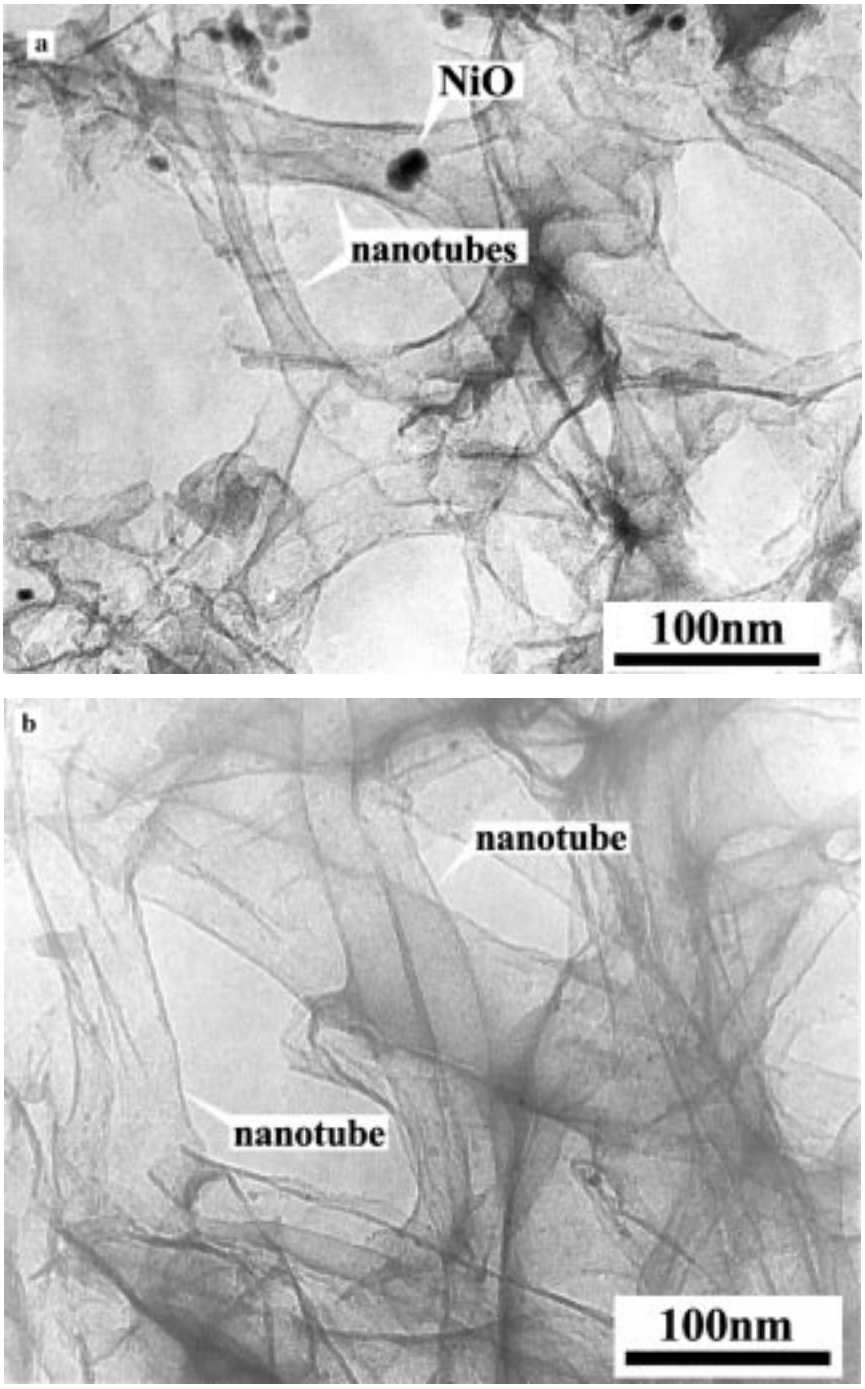

Figure 3. Silica nanotubes (a) and (b).

Another kind of structure is observed when CFC is synthesized by methane decomposition during no more than 6 h on a catalyst with the largest diameter particles (ca. 60 nm). Some structural elements shaped as silica nanotubes are clearly seen in figure 3 (a) and (b). Similar structures were observed earlier [2]. In that study, silica films were supported using the sol–gel method on short carbon nanotubes grown by the plasma method, carbon was then eliminated. However, the specific surface area of such a silica material was as little as 550 m^2/g, probably due to a low density of the starting carbon matrix consisting of nanotubes.

After removal of the carbon, the aerogel prepared by the method under discussion in the present paper is a very porous matrix pierced by passages with nickel oxide particles incorporated in it. The NiO particles are 30–35 nm in average size. The formation of NiO particles of this size is accounted for by the evolution of nickel particles in the course of CFC growth; they merge and disperse to reach the thermodynamically favorable size under the given conditions [37]. Upon burning the carbon, nickel is transformed to the oxide, the particle size being practically unchanged unless the concentration of NiO is not higher than 25%

in the aerogel. Otherwise, silica cannot stabilize dispersed NiO which is sintered to coarser particles. The content of nickel in the aerogel can be controlled by varying the time of carbonization of the initial catalyst and the number of cycles of supporting silica on carbon. The nickel concentration in silica may be varied from 2 to 25%. Notice that apart from NiO particles seen in the micrographs, the silica coats include nickel, which is atomically dispersed during the carbon filament growth. These may be species intermediate between nickel oxide and nickel silicate. These species are highly dispersed, they are not identified by XRD but IR spectra indicate the presence. The silica films constituting the aerogel are extremely thin and comprise the highly dispersed catalytically active metal; therefore, they are expected to reveal an unusually high activity to catalytic reactions.

3.4. Catalytic activity of aerogels to direct oxidation of hydrogen sulfide into sulfur

Comparative studies were carried out using two samples (table 3):

(1) Aerogel containing 7% of nickel oxide prepared by supporting silica on filamentous carbon.

(2) Nickel oxide-free aerogel prepared by supporting silica on Sibunit.

3.4.1. Oxidation of H_2S under stoichiometric conditions

The aerogel with the nickel constituent was found to have much higher activity than the comparative sample. It is seen in figures 4 and 5 that the hydrogen sulfide conversion at 200 °C was 20% on the CFC-templated aerogel against 5% on the Sibunit-templated one; the 100% selectivity to sulfur was observed with both samples. As the reaction temperature increases, the hydrogen sulfide conversion increased slowly at the temperature ranging between 300 and 350 °C to reach a maximum, SO_2 not being detected in the outlet mixture up to 350 °C. At the further temperature elevation, the conversion increased but sulfur dioxide was formed in a considerable proportion.

At 400 °C, the outlet concentration of sulfur dioxide was 0.125% for the CFC-templated aerogel and 0.105% for the Sibunit-templated aerogel. These concentrations are close to the thermodynamically computed values (0.141%) for these conditions. Temperature dependencies of the conversion and selectivity to sulfur determined by thermodynamic computing for the given reaction conditions are plotted in figure 6. Apparently, the hydrogen sulfide conversion can be improved at low temperatures by increasing the contact time of the reactants and the catalyst. The probability of the reverse reaction between elemental sulfur and water increases at above 300 °C which decreases the observed conversion of hydrogen sulfide. Notice that, unlike oxidation of H_2S in excess oxygen, there is no need of controlling the selectivity under the stoichiometric conditions. The high selectivity is accounted for by thermodynamic reasons in this case.

Lines [111] and [200] assigned to NiO are seen in figure 7 presenting the diffraction pattern of the CFC-templated aerogel. The nickel oxide constituent of the aerogel is sulfidized during the reaction to form well crystallized NiS_2. However, analysis of relative intensities of the peaks in the diffraction pattern of the tested sample shows that the composition of the produced sulfide is not fixed and does not correspond to the stoichiometric NiS_2. It is likely to comprise oxygen-containing species.

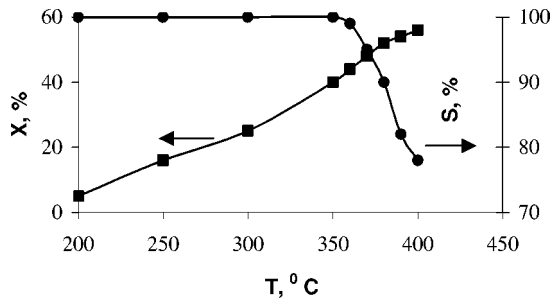

Figure 4. Conversion of hydrogen sulfide (■) and selectivity to sulfur (●) versus temperature. The aerogel was synthesized with Sibunit as the template; inlet gas mixture 1% H_2S + 0.5% O_2 + N_2, consumption of gas mixture 60 cm^3/min.

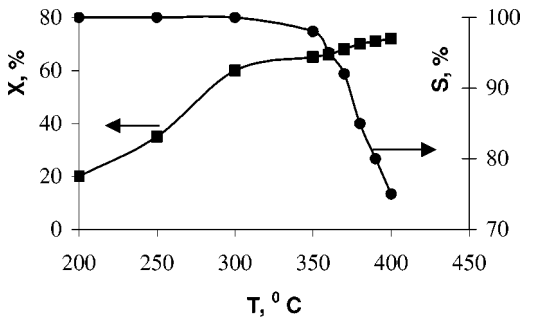

Figure 5. Conversion of hydrogen sulfide (■) and selectivity to sulfur (●) versus temperature. The aerogel was synthesized with CFC as the template; inlet gas mixture 1% H_2S + 0.5% O_2 + N_2, consumption of gas mixture 60 cm^3/min.

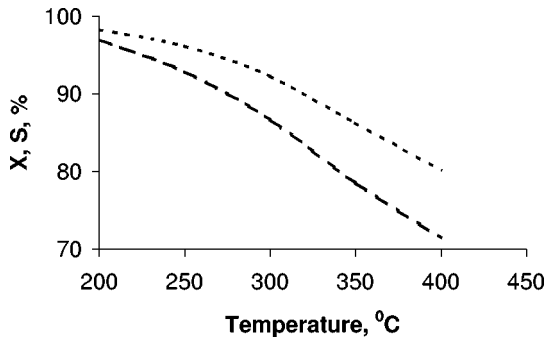

Figure 6. Conversion of hydrogen sulfide (– – –) and selectivity to sulfur (- - -) versus temperature. The temperature dependencies were determined by thermodynamic computing; inlet gas mixture 1% H_2S + 0.5% O_2 + N_2.

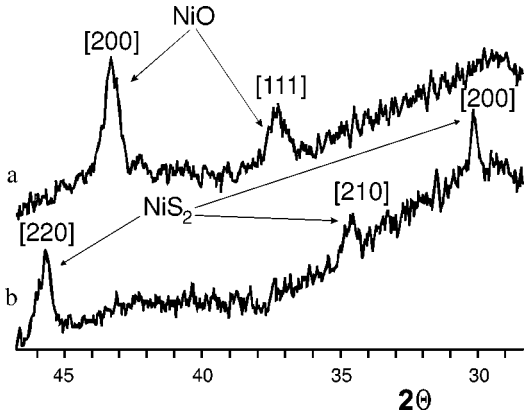

Figure 7. Diffraction patterns of aerogel synthesized by templating CFC with silica: (a) fresh sample and (b) sample after the reaction of oxidation of H_2S into S^0.

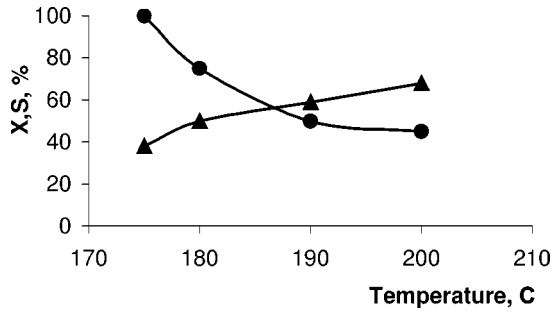

Figure 8. Conversion of hydrogen sulfide (▲) and selectivity to sulfur (●) versus temperature. The aerogel was synthesized with Sibunit as the template; inlet gas mixture 0.5% H_2S + 16% O_2 + N_2, consumption of gas mixture 60 cm^3/min.

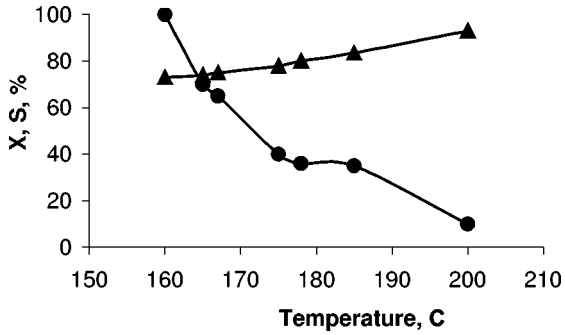

Figure 9. Conversion of hydrogen sulfide (▲) and selectivity to sulfur (●) versus temperature. The aerogel was synthesized with CFC as the template; inlet gas mixture 0.5% H_2S + 16% O_2 + N_2, consumption of gas mixture 60 cm^3/min.

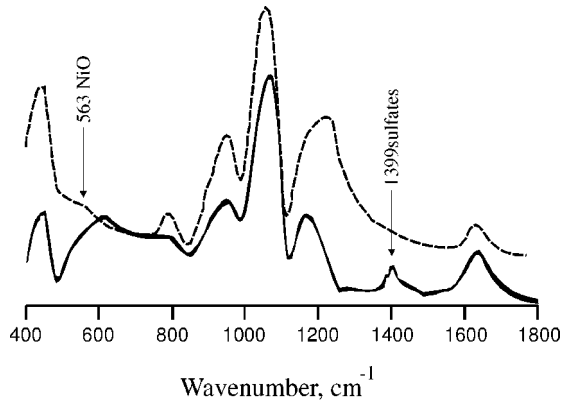

Figure 10. IR spectra of aerogel synthesized by templating CFC with silica recorded before and after the reaction of oxidation of H_2S into S^0. (- - -) Fresh catalyst, (—) spent catalyst.

3.4.2. Oxidation of H_2S in excess oxygen

The activity of the nickel-containing aerogel at both excess oxygen and stoichiometric conditions was much higher than the activity of the Sibunit-templated aerogel. Notice that the hydrogen sulfide conversion increased and the selectivity to sulfur decreased during the early hours of the operation of both catalysts. A high conversion of hydrogen sulfide was observed with both catalysts at 200 °C in the stationary operation mode, while the selectivity to sulfur decreased constantly, i.e., SO_2 was formed. The conversion and selectivity were 80% and 42%, respectively, on the Sibunit-templated aerogel and 93% and 17%, respectively, on the CFC-templated aerogel.

As the reaction temperature decreased, the conversion of hydrogen sulfide decreased and the selectivity to sulfur increased on both catalysts. For example, the selectivity was as high as 100% (no SO_2) and the conversion 39% on the Sibunit-templated aerogel at 175 °C (figure 8). As to the nickel-containing aerogel (figure 9), these characteristics were 100% and 73%, respectively, at 160 °C. The catalyst activity and selectivity did not change during 20 h operation under these conditions. Emphasize that, if the long duration of the reaction was achieved by maintaining the reaction temperature as high as to provide evaporation of sulfur from the reaction zone, a high conversion was attained at the absence of SO_2 among the reaction products. Conventional high-active catalysts, such as nickel oxide, copper oxide and active carbons, produce SO_2 in considerable amount at these temperatures. That is the reason for decreasing the reaction temperature to 100 °C or lower. As a result, sulfur is deposited into the catalyst pores to cause a decrease in the catalytic activity. Periodical catalyst regeneration becomes necessary for regaining the activity that, certainly, deteriorates the process efficiency. For the case under discussion, no change was revealed in the pre- and post-reaction surface area of the catalysts. Thus, no sulfur deposition occurs in the catalyst pores.

XRD study of the CFC-templated aerogel sample shows disappearance of peaks assigned to NiO after completion of the reaction, no other crystal compounds being observed. Therefore, nickel oxide is transformed to roentgen amorphous sulfide or sulfate species. IR spectra of the same sample recorded before and after the reaction are presented in figure 10. The Ni–O bond is detected in the fresh sample and not in the post-reaction sample but the absorption band, which is characteristic of the sulfate, appears. Besides, the shape of peaks assigned to the Si–O bond argues probable transformation of that part of nickel, which is in the form of amorphous silicates, into the sulfur-containing species.

4. Conclusions

The structure of the CFC-templated aerogel prepared by the sol–gel method into the pores of a carbon matrix was studied. BET studies demonstrated that a high specific surface area, which is stable at high temperatures, is characteristic of all the aerogel samples. The surface of these aerogels is mainly built up by mesopores.

The structure of the CFC matrix was shown to influence the structure of the produced aerogel.

High-resolution electron microscopic studies allowed the following structural elements to be revealed in the aerogel samples:

(1) thin-wall matrix pierced by holes (predominant),

(2) silica nanofibers,

(3) silica nanotubes.

All of the CFC-templated aerogels contain nickel oxide particles; besides, nickel as highly dispersed silica species is incorporated into silica.

Investigations of the catalytic activity of the aerogel sample with respect to direct oxidation of hydrogen sulfide into sulfur demonstrated its activity, for both the stoichiometric process and in the presence of a considerable excess of oxygen. This phenomenon may be attributed to the high surface area of the aerogel, which is exposed to the reactants, due to the absence of micropores, as well as to the presence of active metal compounds.

The selectivity to sulfur (100%) observed at the temperatures above the sulfur condensation point (160 °C) in excess oxygen was unusually high for nickel compounds incorporated in the aerogel. A probable reason is that the initial nickel oxide particles are large enough (30–40 nm) to cause a decrease in the NiO activity for oxidation of H_2S into SO_2 but to provide a high selectivity to sulfur.

Acknowledgement

The present work is supported by the Russian Foundation for Basic Research (Grant 99-03-32274).

References

[1] M.T. Anderson, P.S. Samyer and T. Rieker, Micropor. Mesopor. Mater. 20 (1998) 53.
[2] B.C. Satishkumar, F. Govindaraj, E.M. Vogl, L. Basumailick and C.N.R. Rao, J. Mater. Res. 12 (1997) 604.
[3] S. Sakka and K. Kamiya, J. Non-Cryst. Solids 48 (1982) 31.
[4] E.J.A. Pope and J.D. Mackenzie, J. Non-Cryst. Solids 87 (1986) 185.
[5] S. Rajeshkumar, G.M. Anilkumar, S. Ananthakumar and K.G.K. Warrier, J. Porous Mater. 5 (1998) 59.
[6] J.C. Ro and J.J. Chung, J. Non-Cryst. Solids 130 (1991) 8.
[7] A. Ueno, H. Suzuki and Y. Kotera, J. Chem. Soc. Faraday Trans. I 79 (1983) 127.
[8] S. Roy and D. Chakravorty, J. Mater. Res. 8 (1993) 689.
[9] S. Roy and D. Chakravorty, J. Mater. Res. 9 (1994) 2314.
[10] J.P. Wang and H.L. Luo, J. Appl. Phys. 75 (1994) 7425.
[11] V.A. Sviderski, M.G. Voronkov, V.S. Klimenko and S.V. Klimenko, J. Prikl. Khim. 70 (1997) 1698.
[12] G. Ennas, A. Mei, A. Musinu, G. Piccaluga, G. Pinna and S. Solinas, J. Non-Cryst. Solids 232–234 (1998) 587.
[13] B. Ernst, S. Libs, P. Chaumette and A. Kiennemann, Appl. Catal. A 186 (1999) 145.
[14] M.A. Ermakova, D.Yu. Ermakov, G.G. Kuvshinov and L.M. Plyasova, J. Catal. 187 (1999) 77.
[15] M.A. Ermakova, D.Yu. Ermakov, G.G. Kuvshinov, V.B. Fenelonov and A.N. Salanov, J. Porous Mater. 7 (2000) 435.
[16] M.A. Ermakova, D.Yu. Ermakov and G.G. Kuvshinov, Appl. Catal. A, in press.
[17] L.B. Avdeeva, O.V. Goncharova, D.I. Kochubey, B.N. Novgorodov, L.M. Plyasova and Sh.K. Shaikhutdinov, Appl. Catal. A 141 (1996) 117.
[18] G.G. Tibbetts and M.P. Balogh, Carbon 37 (1999) 241.
[19] L.B. Avdeeva and S.K. Shaikhutdinov, in: *EuropaCat-IV*, Rimini, Italy, 5–10 September 1999, p. 559.
[20] M.S. Kim, N.M. Rodriguez and R.T.K. Baker, J. Catal. 131 (1991) 60.
[21] L.B. Avdeeva, D.I. Kochubey and Sh.K. Shaikhutdinov, Appl. Catal. A 177 (1999) 43.
[22] A.A. Khassin, T.M. Yurieva, V.I. Zaikovskii and V.N. Parmon, React. Kinet. Catal. Lett. 64 (1998) 63.
[23] G.G. Kuvshinov, Yu.I. Mogilnykh, D.G. Kuvshinov, D.Yu. Ermakov, M.A. Ermakova, A.N. Salanov and N.A. Rudina, Carbon 37 (1999) 1239.
[24] R.T.K. Baker, in: *Carbon Fibers Filaments and Composites* (Kluwer Academic, Dordrecht, 1999) p. 405.
[25] R.A. Buyanov, V.V. Chesnokov, A.D. Afanasiev and V.S. Babenko, Kinet. Katal. 18 (1977) 1021.
[26] R. Sreeramamurthy and P.G. Menon, J. Catal. 37 (1975) 287.
[27] A. Primavera, A. Trovarelli, P. Andreussi and G. Dolcetti, Appl. Catal. A 173 (1998) 185.
[28] N. Keller, C. Pham-Huu, C. Crouzet, M.J. Ledoux, S. Savin-Poncen, J.B. Nougayrede and J. Bousquet, Catal. Today 53 (1999) 535.
[29] E. Laperdrix, G. Costentin, O. Saur, J.C. Lavalley, C. Nédez, S. Savin-Poncet and J. Nougayrède, J. Catal. 189 (2000) 63.
[30] K.T. Li, C.S. Yen and N.S. Shyu, Appl. Catal. A 156 (1997) 117.
[31] J.H. Uhm, M.Y. Shin, J. Zhidong and J.S. Chung, Appl. Catal. B 22 (1999) 293.
[32] S.W. Chun, J.Y. Jang, D.W. Park, H.C. Woo and J.S. Chung, Appl. Catal. B 16 (1998) 235.
[33] V.B. Fenelonov, V.A. Likholobov, A.Yu. Derevyankin and M.S. Melgunov, Catal. Today 42 (1998) 341.
[34] A. Guinier, *Theorie et Technique de la Radiocristallographie* (Dunod, Paris) p. 956.
[35] A.F. Danilyuk, T.A. Gorodetskaya, G.B. Barannic and V.F. Lyakhova, React. Kinet. Catal. Lett. 63 (1998) 193.
[36] J.F. Goodman and S.I. Gregg, J. Chem. Soc. 2 (1959) 694.
[37] M.A. Ermakova, D.Yu. Ermakov, L.M. Plyasova and G.G. Kuvshinov, Catal. Lett. 62 (1999) 93.